

DOE/NV/11718--120

Bechtel Nevada

DOE/NV/11718-120
UC-702
NOVEMBER 1997

RECEIVED

MAY 11 1998

OSTI

THE
REMOTE
SENSING
LABORATORY

OPERATED BY BECHTEL NEVADA
FOR THE U.S. DEPARTMENT OF ENERGY

**AN AERIAL RADIOLOGICAL SURVEY OF THE
FAULTLESS SITE
AND SURROUNDING AREA**

CENTRAL NEVADA TEST AREA

DISTRIBUTION OF THIS DOCUMENT IS UNLIMITED

MASTER

JAV

DATE OF SURVEY: SEPTEMBER 9-12, 1996

DISCLAIMER

Portions of this document may be illegible electronic image products. Images are produced from the best available original document.

AN AERIAL RADIOLOGICAL SURVEY OF THE FAULTLESS SITE AND SURROUNDING AREA

CENTRAL NEVADA TEST AREA

DATE OF SURVEY: SEPTEMBER 9-12, 1996

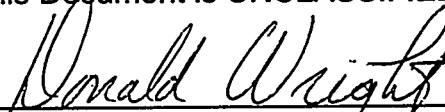
C. M. Bluit
Project Scientist

REVIEWED BY



H. W. Clark, Jr., Manager
Radiation Sciences Section

This Document is UNCLASSIFIED



D. Wright
Authorized Derivative Classifier

ABSTRACT

Terrestrial radioactivity surrounding the Faultless site was measured during September 9–12, 1996, using aerial radiological survey techniques. The purpose of this survey was to document exposure rates near the site and to identify any unexpected man-made radiation sources within the survey area. The surveyed area included land areas within a four-mile (six-kilometer) radius of the site. Data were acquired using an airborne detection system that employs sodium iodide, thallium-activated detectors. Terrestrial exposure-rate and photopeak counts were computed from these data and plotted on maps of the survey area. Terrestrial exposure rates in areas surrounding the site varied from 12–16 microroentgens per hour. No evidence of man-made radiation was detected at the site.

CONTENTS

Abstract	ii
Sections	
1.0 Introduction	1
2.0 Survey Site Description	1
3.0 Survey Methods	1
3.1 Aerial Radiation Measurements	1
3.2 Data-Acquisition System	3
3.3 Detector Characteristics	5
4.0 Data Analysis	5
4.1 Natural Background Radiation	6
4.2 Measured Terrestrial Exposure Rate	6
4.3 Identifying Sources of Man-Made Radiation from Aerial Survey Data	8
4.4 Isotope-Specific Information from Aerial Survey Data	9
4.5 Detection Limits	10
5.0 Aerial Radiological Survey Results	10
Figures	
1 Faultless Survey Site and Surrounding Area	2
2 MBB BO-105 Helicopter with Detector Pods	3
3 Survey Data-Acquisition Techniques	4
4 Typical Background Spectrum of the Faultless Survey Area	7
5 Exposure-Rate Map of the Faultless Site and Surrounding Area	11
B-1 Geometry Used in the Derivation of Conversion Factors Retaining Photopeak Count-Rate Data to Isotopic Concentrations in the Ground	13
Tables	
1 Approximate Detector Footprint Radius for Relative Count-Rate Contributions from Terrestrial Sources at a Survey Altitude of 150 ft (46 m) AGL	6
2 Gamma-Ray Photopeak Identifications—Background Within the Survey Area	7
3 Spectral Regions Used in Net Isotopic Count-Rate Calculations	9
Appendices	
A Survey Parameters	12
B Derivation of Conversion Factors	13
References	16

1.0 INTRODUCTION

An aerial radiological survey of the Faultless site and surrounding area was conducted by the Remote Sensing Laboratory (RSL) for the U.S. Department of Energy (DOE) during September 9–12, 1996. This survey is part of an ongoing effort to characterize radiation levels in areas where detonations occurred in the early 1960s.

The survey consisted of aerial measurements of both natural and man-made gamma radiation emanating from the terrestrial surface. The purpose of this survey was to measure the exposure rates near the site and to determine if measurable contamination had spread outside the site boundaries. Results are reported as radiation isopleths superimposed on topographic maps of the area.

The RSL performs various types of radiological surveys for the DOE and other customers. The RSL capabilities include an airborne radiological surveillance system called the Aerial Measuring System (AMS).¹ Since its inception in 1958, the AMS program has carried out radiological surveys of nuclear power plants, processing plants for nuclear materials, and research laboratories. The AMS aircraft have been deployed to nuclear accident sites and in searches for lost radioactive sources. The AMS aircraft also fly mapping cameras and multispectral camera arrays for aerial photography and thermal mappers for infrared imagery. Survey operations are conducted at the request of various federal and state agencies.

2.0 SURVEY SITE DESCRIPTION

The Faultless survey site is located approximately 55 mi (90 km) northeast of Tonopah, Nevada. Figure 1 shows the Faultless survey site and surrounding area.

The topography consists of both flat and gently rolling desert terrain with mountains located to the north of the site. This area has very little vegetation and is considered open range for livestock.

The survey site is a typical desert region, dry with very little vegetation. It is bordered by a small mountain range and the site ground zero is 6,000 ft (1,830 m) above sea level. The terrain elevations vary from 5,800–7,000 ft (1,770–1,920 m) over a 7-mi (11-km)

area. The main access road, Route 6, is paved and other gravel surface roads lead to the site.

3.0 SURVEY METHODS

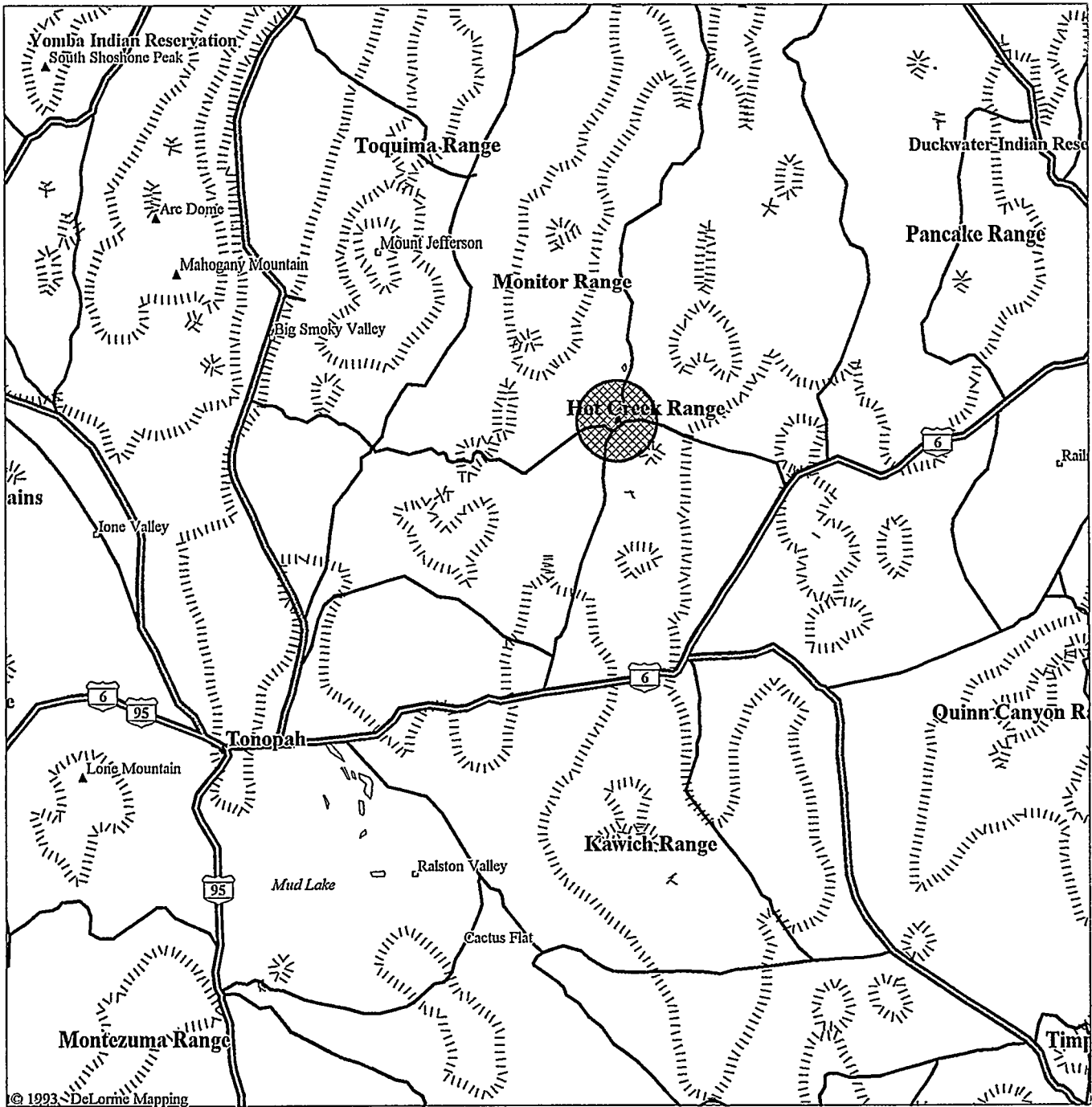
Standard aerial radiation survey techniques developed for large-area gamma radiation surveys were used here.² The survey methodology has been successfully applied to more than 300 individual surveys at various locations beginning in the late 1960s.

3.1 Aerial Radiation Measurements

A Messerschmitt-Bolkow-Blohm (MBB) BO-105 helicopter with externally mounted detector pods, shown in Figure 2, was used to collect the data. Figure 3 illustrates important details of the aerial radiological survey process. Gamma-ray spectral data were acquired at uniform spacing along a series of parallel lines that were flown in a north–south direction at an altitude of 150 ft (46 m) above ground level (AGL) and at a line spacing of 250 ft (76 m). Data were acquired continuously along these lines and recorded at one-second intervals at an airspeed of 70 knots (36 m/s). This one-second interval corresponds to a 118-ft (36-m) data interval. During each interval, two gamma-ray spectra were collected from a single sodium iodide, thallium-activated, NaI(Tl), detector and a series of eight NaI(Tl) detectors. Other information such as position, air temperature, pressure, and altitude were also recorded during each interval.

The helicopter position was established by a Global Positioning System (GPS) operated in differential mode. Real-time aircraft positions were determined by an on-board GPS receiver, based on the measured position from GPS satellite data and a correction transmitted from a second GPS station located at a known position on the ground. The airborne GPS receiver provided continuous positional data to a microprocessor that reformatted the data for use in the RSL airborne computerized data-logging systems. This on-board computer recorded the positional data and operated a steering indicator to aid the pilot in flying a set of equally spaced straight lines.

Real-time altitude measurements were made through a radar altimeter that measured the return time for a pulsed signal and converted this delay to aircraft altitude. For altitudes up to 2,000 ft (610 m), the manufacturer's stated accuracy is ± 2 ft (0.6 m) or ± 2 percent,



© 1993 DeLorme Mapping

Road and Place Map From DeLorme XMap® Professional

LEGEND

- Geo Feature
- ◆ Town, Small City
- ▲ Hill
- ⬮ US Highway
- Major Street/Road
- == State Route
- == US Highway
- ||||| Contour

- Land
- Open Water

Scale 1:1,000,000 (at center)

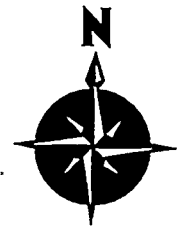
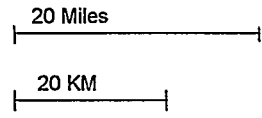


FIGURE 1. FAULTLESS SURVEY SITE AND SURROUNDING AREA. The red, cross-hatched region represents the aerial survey area. The red dot inside the red, cross-hatched region represents the Faultless site ground zero.



FIGURE 2. MBB BO-105 HELICOPTER WITH DETECTOR PODS

whichever is greater. Altitude data were also recorded by the data-acquisition system so that variations in gamma signal strength caused by altitude fluctuations could be identified.

3.2 Data-Acquisition System

The detection system consists of two rectangular aluminum pods. Each pod contains four 2- × 4- × 16-in down-looking and one 2- × 4- × 4-in up-looking NaI(Tl) scintillation detectors. Pulse inputs from the eight 2- × 4- × 16-in detectors were summed and recorded as a spectrum, as discussed below. In addition, a spectrum from one of the 2- × 4- × 16-in detectors was recorded separately to provide increased dynamic range when viewing high-radiation areas. Counts from only the 2- × 4- × 4-in detector were recorded for possible use in a correction for nonterrestrial radiation contributions. The 2- × 4- × 16-in detectors were surrounded by thermal-insulating foam and shielded on the top and sides by 0.03-in (0.076-cm) cadmium and lead sheets. The 2- × 4- × 4-in detectors were shielded on the bottom and sides by the cadmium and lead sheets.

Spectral data were acquired and displayed in real time using specialized instrumentation that processes, stores, and displays spectral data. This system was developed for aerial radiological surveys and contains the necessary instrumentation in a single package. The system, called Radiation and Environmental Data Acquisition and Recorder, Version IV, (REDAR IV) system, is a multi-microprocessor, portable data-acquisition, and real-time analysis system.³ It has been designed to operate in the severe environments

associated with platforms such as helicopters, fixed-wing aircraft, and various ground-based vehicles. The system displays the required radiation and system information to the operator, in real time, through the display of a cathode-ray tube (CRT) and through multiple readouts. Pertinent data were recorded on cartridge tapes for later analysis.

The REDAR IV system contains six subsystems: (a) two independent radiation data-collection systems, (b) a general purpose data input/output (I/O) system, (c) a tape recording/playback system, (d) a CRT display system, (e) a real-time data-analysis system, and (f) a ranging system with steering calculation and display capabilities. These subsystems, which are under the operator's control, handle functions including data collection, analysis, and display; positional and steering calculations; and data recording.

Two multichannel analyzers (MCA) in the REDAR IV system collect 1,024-channel gamma-ray spectra (4.0 keV per channel) once every second during the survey operation. The primary MCA (for the eight-detector spectrum) has a usable dynamic range to about 100,000 counts per second (cps) corresponding to an exposure rate of about 1.5 milliroentgens per hour (mR/h) at one meter AGL. Spectral information at high-count rates begins to degrade at approximately half this rate; a single NaI(Tl) detector and second MCA are used when the system is used in high-count-rate situations.

The data-acquisition system is calibrated to a 0–4,000-keV energy range using gamma-ray sources of americium-241 (²⁴¹Am) at 60 keV; sodium-22 (²²Na) at 1,275 keV; and cesium-137 (¹³⁷Cs) at 662 keV. A 28-keV low-energy threshold is selected to minimize counts from the lower part of the continuum. The summed signal derived from the eight NaI(Tl) detectors was adjusted prior to processing by the analog-to-digital converter so that the calibration peaks appeared in preselected channels in the MCA of the data-acquisition system.

Because the energy resolution of NaI(Tl) crystals decreases with increasing energy, spectra are compressed to conserve storage space. Spectra are divided into three partitions where the detected photopeak width is approximately the same. Data in the first partition (0–300 keV) are not compressed to permit stripping of low-energy photopeaks such as the

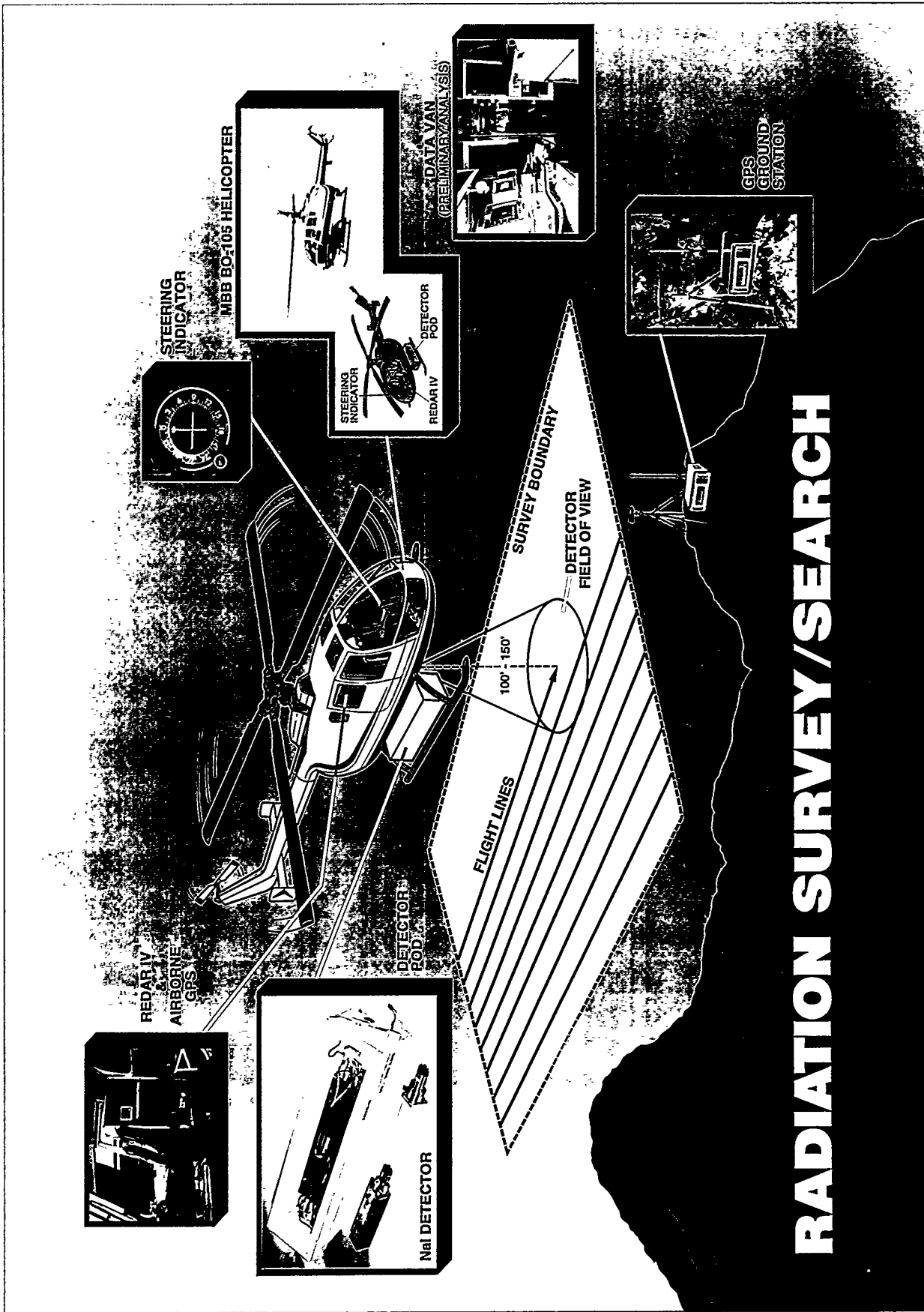


FIGURE 3. SURVEY DATA-ACQUISITION TECHNIQUES

60-keV photopeak from ^{241}Am . The second partition (300–1,620 keV) is compressed to 12 keV per channel while the third partition (1,620–4,000 keV) is compressed to 36 keV per channel. The spectral compression technique reduces the amount of data storage required by a factor of four.

Two full spectra, one spectrum containing data from the eight detectors and a second spectrum containing data from a single detector, and related information such as position, time, and air temperature are recorded every second. The REDAR IV system has two sets of spectral memories; each memory can accumulate four individual spectra. The two memories support continuous data accumulation: one memory stores data while the other memory transfers data to magnetic tape. At a survey speed of 70 knots (36 m/s), 45 data sets were acquired for each mile of flight.

3.3 Detector Characteristics

The detector system was designed to sense terrestrial and airborne gamma radiation having energies between 20 and 4,000 keV. This energy range includes emitted gamma radiation from naturally occurring radionuclides and almost all man-made gamma radiation sources.

NaI(Tl) detectors used in this survey are characterized by their variable sensitivity versus incident gamma energy and by a footprint size that is also energy-dependent. The variation in sensitivity with incident energy is a well-known characteristic of NaI(Tl) detectors. Detailed data on detector sensitivity can be obtained from the manufacturer.⁴ The dependence of the viewed footprint size with energy can be modeled. Because of the large footprint, sources detected by the aerial systems appear to be spread over a much larger area than would be indicated by ground-based measurements.

For uncollimated detectors such as those used in this aerial survey, the source-to-detector distance and the attenuation by the air effectively limit the size of the viewed terrestrial area to a circular region centered directly beneath the detector. The size of the field of view is a function of the gamma-ray energy, the gamma-ray origin, and the detector response. Radionuclide activities on or in the soil and exposure rates

normalized to one meter AGL are customarily reported but only as large-area averages. Activity inferred from aerial data for a source uniformly distributed over a large area compared to the field of view of the detectors is very good and generally agrees with ground-based measurements. However, activity for a point source, a line source, or a source area less than the detector's field of view will be underestimated, sometimes by orders of magnitude. When this occurs, the aerial data simply serve to locate and identify such sources.

Apparent source-broadening makes comparison with ground-based measurements difficult. Radionuclides that occur as hot particles are averaged by the aerial detection system, appearing as uniform large-area distributions. Ground surveys, however, would locate the hot particles within a smaller area and show the surrounding areas to be free of contamination. Table 1 contains estimates of the detection system's field of view or "footprint" size for several energies of interest.

Detector sensitivity is not constant throughout the footprint. The maximum sensitivity occurs directly beneath the detector; the sensitivity decreases with increasing horizontal distance between the source and airborne detector. In addition, the incident gamma rays from even a monoenergetic source include scattered gamma rays once the incident radiation reaches the airborne detectors. Footprint sizes are therefore dependent on the source location: distributed in the soil, scattered by passing through air, inside a container, etc.

4.0 DATA ANALYSIS

Data processing was initiated in the field using a computer analysis laboratory installed in a mobile van located near the survey site. Before leaving the site, data were examined and a preliminary analysis was completed to ensure that the raw data were satisfactory.

Standard techniques for analyzing survey data were used: terrestrial exposure rates were computed from gross count data with a correction for variations in altitude. Man-made radioactivity, ^{137}Cs , and cobalt-60 (^{60}Co) activity were determined through differences between total counts in appropriate spectral windows.⁵

Table 1. Approximate Detector Footprint Radius for Relative Count-Rate Contributions from Terrestrial Sources at a Survey Altitude of 150 ft (46 m) AGL

Emitted Gamma-Ray Energy (keV)	Radius where 99% of Detected Counts Originate ft (m)	Radius where 90% of Detected Counts Originate ft (m)	Radius where 50% of Detected Counts Originate ft (m)
60	650 (198)	353 (108)	155 (47)
200	850 (259)	435 (133)	178 (54)
600	1,067 (325)	560 (171)	214 (65)
1,500	1,715 (523)	772 (235)	260 (79)
2,000	2,145 (654)	850 (259)	275 (84)
3,000	2,862 (872)	1,007 (307)	308 (94)

4.1 Natural Background Radiation

Natural background radiation originates from (a) radioactive elements present in the earth, (b) airborne radon, and (c) cosmic rays entering the earth's atmosphere from space. Natural terrestrial radiation levels depend on the type of soil and bedrock immediately below and surrounding the point of measurement. Within cities, the levels are also dependent on the nature of the pavement and building materials. The gamma radiation originates primarily from the uranium and thorium decay chains and from radioactive potassium. Local concentrations of these nuclides produce radiation levels at the surface of the earth typically ranging from 1–15 $\mu\text{R/h}$ (9–130 mrem/yr). Some areas with high concentrations of uranium and/or thorium in the surface minerals exhibit even higher radiation levels, especially in the western states.⁶ The peaks listed in Table 2 were found in the natural background spectrum. Figure 4 shows a typical spectrum from natural background within the Faultless survey area.

Isotopes of the noble gas radon are members of both the uranium and thorium radioactive decay chains. Radon can diffuse through the soil and may travel through the air to other locations; therefore, the level of airborne radiation due to these radon isotopes and their daughter products at a specific location depends on a variety of factors, including meteorological conditions, mineral content of the soil, and soil permeability.

Typically, airborne radon contributes from 1–10 percent of the natural background radiation.

Cosmic rays interact with elements of the earth's atmosphere and soil. These interactions produce an additional natural source of gamma radiation. Radiation levels due to cosmic rays vary with altitude and geomagnetic latitude. Typically, values range from 3.3 $\mu\text{R/h}$ at sea level in Florida to 12 $\mu\text{R/h}$ at an altitude of 1.9 mi (3 km) in Colorado.⁷

4.2 Measured Terrestrial Exposure Rate

The measured count rate in the aircraft differs from the true terrestrial exposure rate due to background sources in the aircraft: (a) variation of cosmic radiation with altitude, (b) temporal variation in atmospheric radon concentration, and (c) attenuation by the air of gamma rays emitted from the ground. Because the raw count-rate data over the survey area have been found to vary with time, data from each flight were normalized to data measured over a fixed test line, which was measured at the beginning and end of each data-acquisition flight. This normalization was used to minimize the effects of variations in the natural airborne and aircraft background radiation. A test line was selected for this survey.

The terrestrial exposure rate can be calculated as follows:

Table 2. Gamma-Ray Photopeak Identifications—Background Within the Survey Area

Energy (keV)	Identification
240	^{208}Tl (239 keV), ^{212}Pb (238 keV)
380	^{228}Ac (339 keV), ^{214}Bi (387keV, 389 keV)
511 (weak)	^{208}Tl (511 keV), annihilation
610	^{214}Bi (609 keV)
830 (weak)	^{228}Ac (795 keV), ^{208}Tl (861 keV)
930	^{228}Ac (911 keV), ^{214}Bi (934 keV)
1,130	^{214}Bi (1,120 keV)
1,230	^{214}Bi (1,238 keV)
1,460	^{40}K (1,460 keV)
1,750	^{214}Bi (1,765 keV)
2,160	^{214}Bi (2,204 keV)
2,560	^{208}Tl (2,614 keV)

$$\text{Exposure Rate} = (\text{Conversion Factor}) \cdot (GC - B) \cdot e^{-(A \cdot \text{altitude})} \quad (1)$$

GC is the gross count rate (sum of the contents of all spectrum channels) recorded by the REDAR IV system, and A and B are constants. A is the site-specific atmospheric attenuation coefficient and has been found to be constant over the duration of a survey. A

is determined from data taken at multiple altitudes over the test line. B represents the nonterrestrial background count rate and is calculated from test-line count rates measured before and after each survey data flight (using the previously determined value of A). An average value of B , the recorded altitude at each data interval, and the value of A are used to correct all measurements to yield the correct terrestrial gamma-emission rate. (Such a correction could be gamma-ray energy-dependent. At present, it is assumed that the relative contributions to the measured spectrum do not vary between the test line and the survey area, so an average correction is appropriate.)

A three-point sliding interval average was applied to gross count-rate data to reduce statistical fluctuations in the data:

$$c(E)_{i,avg} = [c(E)_{i-1} + c(E)_i + c(E)_{i+1}] / 3 \quad (2)$$

The averaged value at the i th location is $c(E)_{i,avg}$, and $c(E)_{i-1}$, $c(E)_i$, and $c(E)_{i+1}$ are consecutive, corrected gross count rates along a single flight line. Present analysis codes do not average nearest-neighbor data on adjacent flight lines; three-point averaging has been found to be adequate. The exposure rate is calculated from this averaged gross count

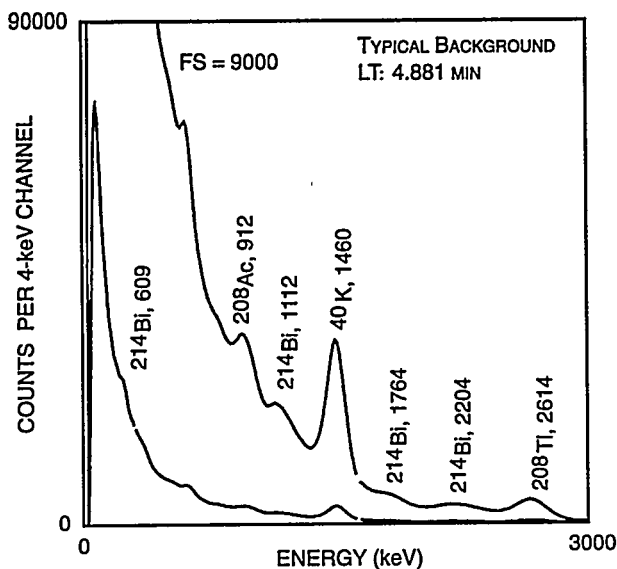


FIGURE 4. TYPICAL BACKGROUND SPECTRUM OF THE FAULTLESS SURVEY AREA

rate. Three-point, sliding interval averaging was applied to man-made and net isotopic data prior to calculating radiation contour maps.

The conversion factor, relating count rates to exposure rates, has been determined in several ways. It can be determined empirically by comparing ground-based exposure-rate measurements with count rates from the airborne system. This was done for the Faultless survey using data obtained from comparative ground-based and aerial measurements of a well-characterized reference line. Two reference lines are maintained for survey calibration: one in Calvert County, Maryland, and a second in the Lake Mohave National Recreation Area near Las Vegas, Nevada. Data from the Lake Mohave Test Line were used for the Faultless survey because the Lake Mohave terrain is similar to the area covered by this survey. A conversion factor of $1.04 \times 10^{-3} \mu\text{R/h (cps)}^{-1}$ was used in the Faultless survey.⁸

The terrestrial exposure-rate isopleth plots are also used as a quality check on the systematic variability of survey data. In particular, exposure-rate isopleths that fall along flight lines, especially along the initial or final lines of individual flights, indicate instability in the detection system. Such variations must be corrected before the data are used. If they cannot be corrected, the uncertainty (error bars) applied to the isopleth plots must be increased to eliminate obvious systematic variations.

4.3 Identifying Sources of Man-Made Radiation from Aerial Survey Data

Contaminated sites are located from isopleth maps based on a man-made radiation source algorithm, referred to as the man-made gross count (MMGC). This analysis provides a general overview of contamination within the survey area and also indicates the areas that should be further investigated. The MMGC algorithm is based on several observations: (a) commonly occurring man-made sources emit gamma rays having energies less than 1,394 keV while natural background sources emit gamma rays both below

and above this threshold and (b) the spectrum continuum shape is relatively constant throughout the survey area. Moreover, gamma rays detected after being scattered (*i.e.*, emitted by sources buried in soil or through atmospheric scattering) will contribute to the continuum at energies below their initial energies.

The measured spectral shape is constant over the survey area assuming (a) a stable cosmic-ray emission rate; (b) a constant background due to the aircraft, airborne radon, and natural sources; and (c) a survey area where the gamma sources and soil composition change relatively slowly in comparison to the area contributing to the measured spectrum. Experience has shown that these assumptions are reasonable within statistical uncertainties over large uncontaminated survey areas. (Significant changes in the source characteristics will invalidate this assumption. For example, changes in the MMGC are seen in spectra acquired over different terrain and when airborne radon levels change.)

If there were no systematic errors in the detection system, the sum of all gamma radiation due to man-made sources would be the difference between the spectrum in question and a typical background spectrum. Unfortunately, systematic errors make this simple subtraction impractical. A more reliable comparison can be made using the ratios of the sum of all channel contents of the spectral region from 38–1,394 keV (the region of man-made gamma emitters) to the sum of the spectral region from 1,394–3,026 keV (the region containing mostly counts from naturally occurring gamma emitters).

$$MMGC = \sum_{E=38 \text{ keV}}^{1394 \text{ keV}} c(E) - \left[K_{MMGC} \cdot \sum_{E=1394 \text{ keV}}^{3026 \text{ keV}} c(E) \right] \quad (3)$$

The contents of spectrum channels corresponding to energies within the range of summation are represented by $c(E)$. The MMGC is the difference for a spectrum measured over an area containing man-made radionuclides, computed using the previously determined normalization constant, K_{MMGC} . The constant is computed from data measured over areas free of contamination as follows:

$$K_{MMGC} = \frac{\sum_{E=38 \text{ keV}}^{1394 \text{ keV}} c(E)}{\sum_{E=1394 \text{ keV}}^{3026 \text{ keV}} c(E)} \quad (4)$$

Normalization constant values are derived from the data of each flight to minimize the effects of airborne radon-222 (^{222}Rn) and minor system characterization differences between flights.

4.4 Isotope-Specific Information from Aerial Survey Data

While the MMGC provides an indication of radioactive contamination, nuclide-specific information is important for such activities as identifying contamination sources and site remediation. Aerial survey data are also examined for spectral peaks due to various radionuclides that could be reasonably expected to be present at the survey site: ^{60}Co and ^{137}Cs .

Spectral-stripping techniques were used to analyze aerial radiation data. (Peak fitting is not used because peak shapes from the NaI[Tl] detectors are broad and frequently overlap.) Spectra from areas of interest (usually those with significant MMGC levels) are analyzed by subtracting, channel-by-channel, a spectrum of a known background area. These spectra are sums of all spectral data acquired within the area:

$$c_{diff}(E) = c_{site \text{ of interest}}(E) - K_{diff} \cdot c_{background}(E) \quad (5)$$

The K_{diff} constant is selected to force the difference spectrum to zero at the high-energy side. Spectral peaks are readily visible in the difference or net spectrum. The presence of an identifiable spectral peak is considered to be a requirement for proceeding with isotopic contour plots. Once identified, contour plots of individual radionuclides are computed using two- or three-spectral window-stripping techniques on each data spectrum acquired during the survey as follows:

$$c_{Net} = \sum_{E=E_1}^{E_2} c(E) - (K_3) \cdot \left[\sum_{E=E_3}^{E_4} c(E) + \sum_{E=E_5}^{E_6} c(E) \right] \quad (6)$$

The spectrum channel contents are represented by $c(E)$, and E_i represents the limiting energy ranges of the windows. Again, the scaling factor, K_3 , is adjusted to set the isotopic net count to zero for data from known background regions. Spectral-window ranges used for isotopic data presented in this report are shown in Table 3.

Nuclide-specific conversion factors take into consideration the isotopic branching ratios, the spectral-window analysis, and an assumed distribution of the source in the soil. The assumed distribution and soil attenuation at the gamma-ray energy being analyzed clearly affect the calibration. An assumed distribution of radionuclides is often a best estimate leading to an unavoidable uncertainty in the computed soil activity. Contamination may be dispersed on the surface, with no contamination below the surface, or distributed

Table 3. Spectral Regions Used in Net Isotopic Count-Rate Calculations

Isotope	Peak Region (keV)	First Background Region (keV)	Second Background Region (keV)
^{137}Cs	590 – 734	506 – 590	734 – 794
^{60}Co	1,094 – 1,394	1,394 – 3,026	—

throughout the soil. The latter case has been found to be more probable.

4.5 Detection Limits

Aerial radiological survey results provide information about radiation levels at the site and in the surrounding area (generally a relatively constant background). Due to the large survey footprint, aerial data are only an approximate measure of the extent of site-based radioactivity.

Aerial radiological survey data consist of many single measurements distributed over the survey area. It has been found from previous surveys that the survey data always contain large regions of average back-

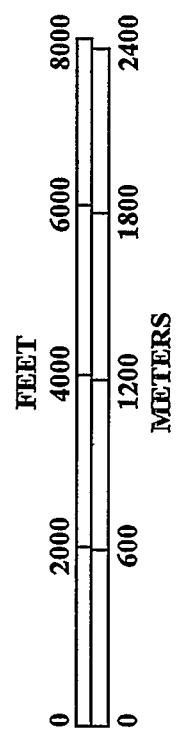
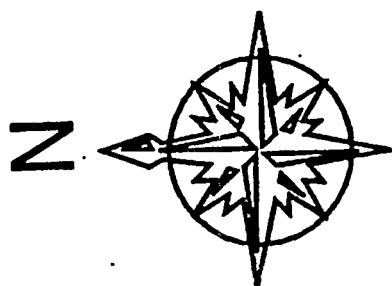
ground radiation with a few anomalous locations (*i.e.*, background areas slightly higher or lower than average, site-related radioactivity, etc.).

5.0 AERIAL RADIOLOGICAL SURVEY RESULTS

Radiation isopleth plots were made of the Faultless site for exposure rate. The plot showed no unusual activity around the site, as expected.

Figure 5 is a plot of the terrestrial exposure rates over the Faultless site. The contribution from cosmic rays and airborne radon has been removed. There were no other high-exposure-rate areas detected in the surrounding survey area.





CONVERSION SCALE	
Color Code	Exposure Rate ^a (μR/h)
	< 12
	12 - 14
	16 - 18

^aThe exposure rate is inferred from the count-rate data collected at an altitude of 150 ft (46 m) AGL. The listed values do not include an estimated cosmic-ray exposure rate of 6.5 μR/h.

FIGURE 5. EXPOSURE-RATE MAP OF THE FAULTLESS SITE AND SURROUNDING AREA

APPENDIX A
SURVEY PARAMETERS

Survey Site:	Faultless
Survey Location:	Approximately 55 mi (90 km) northeast of Tonopah, Nevada
Survey Date:	September 9–12, 1996
Survey Coverage:	4.0 sq mi (10 sq km)
Survey Altitude:	150 ft (46 m)
Aircraft Speed:	70 knots (41 m/s)
Line Spacing:	250 ft (76 m)
Line Length:	2 mi (3 km)
Line Direction:	North–South
Number of Lines:	Approximately 83
Detector Array:	Eight 2- × 4- × 16-in Na(Tl) detectors Two 2- × 4- × 4-in Na(Tl) detectors
Acquisition System:	REDAR IV
Aircraft:	MBB BO-105 helicopter (Tail Number N40EG)
Project Scientist:	C. M. Bluit

APPENDIX B
DERIVATION OF CONVERSION FACTORS

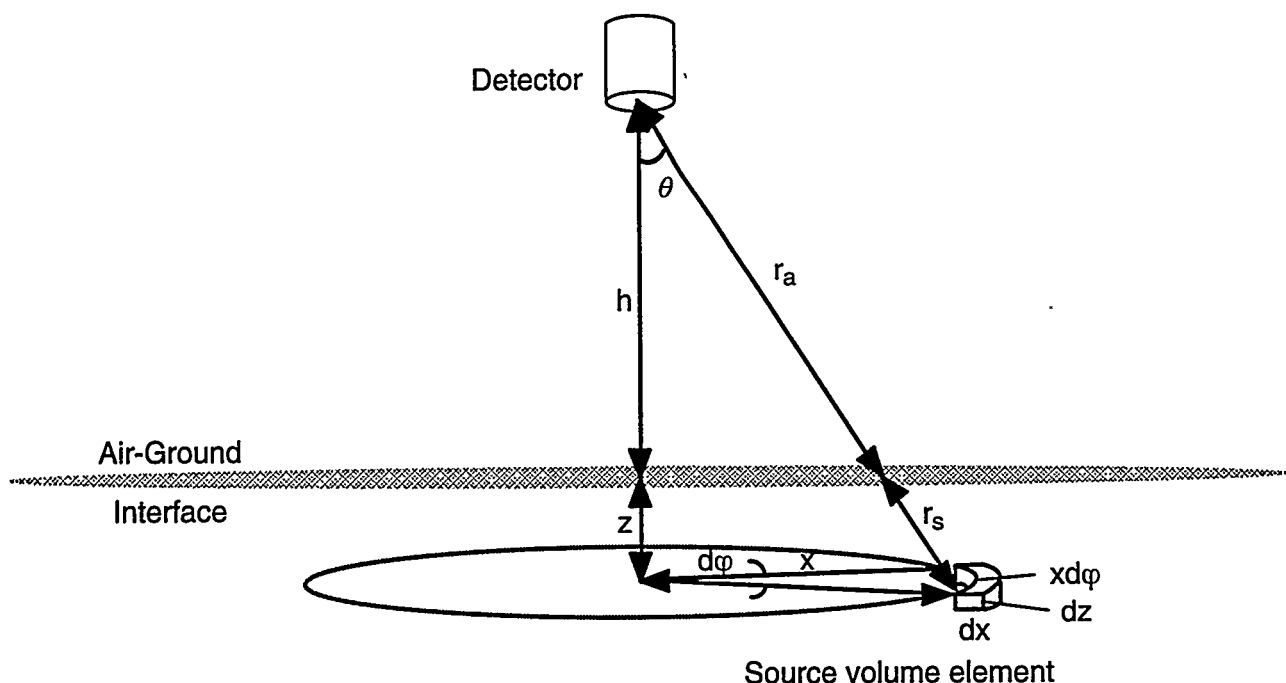


FIGURE B-1. GEOMETRY USED IN THE DERIVATION OF CONVERSION FACTORS RETAINING PHOTOPEAK COUNT-RATE DATA TO ISOTOPIC CONCENTRATIONS IN THE GROUND

The relationship between the photopeak net count rate observed at a distance h above the surface and the activity of a monoenergetic gamma emitter distributed in the soil can be written as follows:⁹

$$\phi = \int_0^{\infty} \int_0^{\infty} \frac{S_V(z)}{4\pi D^2} e^{-\left(\frac{\mu}{\rho}\right)_a \rho_a r_a} e^{-\left(\frac{\mu}{\rho}\right)_s \rho_s r_s} 2\pi x \, dx \, dz \quad (\text{B-1})$$

where

ϕ = photopeak flux at the detector

$S_V(z)$ = activity per unit volume; usually assumed to be a function of depth in the soil
[(γ/s)/ cm^3]

D = detector-to-source distance in the air and the soil combined (cm); $r_a + r_s$

z = source distribution depth in the soil (cm)

x = integration variable; $D = [x^2 + (h+z)^2]^{1/2}$

$(\mu/\rho)_a, (\mu/\rho)_s$ = air and soil mass attenuation coefficients for the monoenergetic gamma energy
(cm^2/g)

ρ_a, ρ_s = air and soil density (g/cm^3)

For man-made radioactive material distribution patterns, the distribution of a gamma emitter in the soil can be approximated by an exponential vertical distribution of concentration:

$$S_V(z) = S_{V0} e^{-\alpha z} \quad (\text{B-2})$$

S_{V0} is the activity per gram of soil at the surface, and α is the reciprocal of the relaxation depth. This implies that the representative volume of soil at a relaxation depth of $1/\alpha$ contains approximately 63 percent of the source's total activity. At relaxation depths of $2/\alpha$ and $3/\alpha$, the representative volume of soil contains approximately 86 and 95 percent, respectively, of the total activity.

The effective area, A , represents the detector's capability or efficiency in detecting the specific gamma ray.

$$N_p = A \phi \quad (\text{B-3})$$

N_p is the photopeak net count rate. The effective area, in general, varies as a function of the gamma-ray angle incident to the detector face and can be written as follows:

$$A = A_0 R(\theta) \quad (\text{B-4})$$

A_0 is the detector-effective area for a unit flux perpendicular to the detector face (zero degrees) (cm^2). $R(\theta)$ is the ratio of the detector response at an angle θ to its response at zero degrees. In practice, the effective area is measured with point radiation sources of different energies whose activities are traceable to the National Institute of Standards and Technology.

Rewriting Equation B-1 in terms of θ and z and combining Equation B-4 leads to an expression that relates the measured photopeak count rate to the source activity where the conversion factor can be expressed in units of $\text{cps}/(\gamma/\text{cm}^3\text{-s})$.

$$\frac{N_p}{S_{V0}} = \frac{A_0}{2} \int_0^{\pi/2} R(\theta) \tan \theta \frac{e^{-\left(\frac{\mu}{\rho}\right)_a \rho_a h \sec \theta}}{\alpha + \left(\frac{\mu}{\rho}\right)_s \rho_s \sec \theta} d\theta \quad (\text{B-5})$$

For a specific isotope, the conversion factor can be changed to units of $\text{cps}/(\text{pCi}/\text{cm}^3)$ by converting gamma rays per second into pCi. This conversion depends on the branching ratio, β , which is the number of gamma rays emitted per disintegrations. Multiplying the expression in Equation B-5 by the soil density (g/cm^3), the conversion factor can be given in units of $\text{cps}/(\text{pCi}/\text{g})$.

The average radionuclide concentration in the top z cm in the soil can be written for an exponentially distributed gamma emitter as follows:

$$S_V^z = \frac{1}{z} \int_0^z S_{V0} e^{-az} dz = \frac{S_{V0}}{az} (1 - e^{-az}) \quad (\text{B-6})$$

By substituting Equation B-6 into Equation B-5 and dividing by the soil density, the conversion factor can be expressed in units of (pCi/g)/cps as follows:

$$\frac{\left(\frac{S_V^z}{\rho_s}\right)}{N_p} = \frac{(1 - e^{-az})}{a z} \beta \left[\frac{A_0 \rho_s}{2} \int_0^{\frac{\pi}{2}} R(\theta) \tan \theta \frac{e^{-\left(\frac{\mu}{\rho}\right)_a \rho_a h \sec \theta}}{a + \left(\frac{\mu}{\rho}\right)_s \rho_s \sec \theta} d\theta \right]^{-1} \quad (\text{B-7})$$

Examples of computed minimum detectable activities and conversion factors for soil concentration from point radiation sources can be found in the literature.^{10,11}

REFERENCES

1. Boyns, P.K. *The Aerial Radiological Measuring System (ARMS): Systems, Procedures and Sensitivity (1976)*. Report No. EGG-1183-1691, 1976; EG&G, Las Vegas, Nevada.
2. Jobst, J.E. "Recent Advances in Airborne Radiometric Technology," *Remote Sensing Technology, Proceedings of a Symposium on Remote Sensing Technology in Support of the United States Department of Energy, 23-25 February 1983*. Report No. EGG-10282-1057, 1985; pp 1-1 to 1-17. EG&G/EM, Las Vegas, Nevada.
3. *Radiation, Environmental Data Acquisition and Recorder System (REDAR IV) Manual*. 1981; Aerial Measurements Operations, EG&G, Las Vegas, Nevada.
4. Belian, J.; R. Dayton. *NaI(Tl) Scintillation Detectors*. Bicron Corporation.
5. Hendricks, T.J. "Radiation and Environmental Data Analysis Computer (REDAC) Hardware, Software, and Analysis Procedures," *Remote Sensing Technology, Proceedings of a Symposium on Remote Sensing Technology in Support of the United States Department of Energy*. Report No. EGG-10282-1057, 1985; pp 2-1 to 2-28. EG&G/EM, Las Vegas, Nevada.
6. Lindeken, C.L.; K.R. Peterson; D.E. Jones; R.E. McMillen. "Geographical Variations in Environmental Radiation Background in the United States," *Proceedings of the Second International Symposium on the Natural Radiation Environment, August 7-11, 1972, Houston, Texas, 1972*; pp 317-332. National Technical Information Service, Springfield, Virginia.
7. Klement, Jr., A.W.; C.R. Miller; R.P. Minx; B. Shleien. *Estimates of Ionizing Radiation Doses in the United States, 1960-2000*. U.S. EPA Report ORP/CSD72-1, 1972; EPA, Washington, D.C.
8. Mohr, R.A. *Ground Truth Measurements at the Calvert County, Maryland, Test Line*. Report No. EGG -10282-2066, 1985; EG&G/EM, Santa Barbara, California.
9. Tipton, W.J.; A.E. Fritzsche; R.J. Jaffe; A.E. Villaire. *An In Situ Determination of ²⁴¹Am on the Enewetak Atoll*. Report No. EGG-1183-1778, 1981; EG&G, Las Vegas, Nevada.
10. Beck, H.L.; J. DeCampo; C. Gogolak. *In Situ Ge(Li) and NaI(Tl) Gamma Ray Spectrometry*. Report No. HASL-258, TID-4500, 1972; U.S. AEC Health and Safety Laboratory, New York, New York.
11. Reiman, R.T. *In Situ Surveys of the U.S. Department of Energy's Rocky Flats Plant, Golden, Colorado*. Report No. EGG-10617-1129, 1991; EG&G/EM, Las Vegas, Nevada.